Mon. Not. R. Astron. Soc. **396,** 2051–2060 (2009) doi:10.1111/j.1365-2966.2009.14932.x

The velocity dispersion and mass-to-light ratio of the remote halo globular cluster NGC 2419

H. Baumgardt,[1⋆] P. Côté,[2] M. Hilker,[3] M. Rejkuba,[3] S. Mieske,[4] S. G. Djorgovski[5] and Peter Stetson[2]

[1]*Argelander-Institut für Astronomie, Universität Bonn, Auf dem Hügel 71, 53121 Bonn, Germany*
[2]*National Research Council of Canada, Herzberg Institute of Astrophysics, 5071 West Saanich Road, Victoria, BC V9E 2E7, Canada*
[3]*European Southern Observatory, Karl-Schwarzschild-Strasse 2, 85748 Garching bei München, Germany*
[4]*European Southern Observatory, Alonso de Córdova 3107, Vitacura, Casilla 19001, Santiago, Chile*
[5]*Astronomy Department, California Institute of Technology, MC 105-24, Pasadena, CA 91125, USA*

Accepted 2009 April 15. Received 2009 March 24; in original form 2009 January 26

ABSTRACT

Precise radial velocity measurements from high-resolution echelle spectrometer on the Keck I telescope are presented for 40 stars in the outer halo globular cluster NGC 2419. These data are used to probe the cluster's stellar mass function and search for the presence of dark matter in this cluster. NGC 2419 is one of the best Galactic globular clusters for such a study due to its long relaxation time ($T_{\rm r0} \approx 10^{10}$ yr) and large Galactocentric distance ($R_{\rm GC} \approx 90$ kpc) – properties that make significant evolutionary changes in the low-mass end of the cluster mass function unlikely. We find a mean cluster velocity of $\langle v_{\rm r} \rangle = -20.3 \pm 0.7\,{\rm km\,s^{-1}}$ and an internal velocity dispersion of $\sigma = 4.14 \pm 0.48\,{\rm km\,s^{-1}}$, leading to a total mass of $(9.0 \pm 2.2) \times 10^5\,{\rm M}_\odot$ and a global mass-to-light ratio of $M/L_V = 2.05 \pm 0.50$ in solar units. This mass-to-light ratio is in good agreement with what one would expect for a pure stellar system following a standard mass function at the metallicity of NGC 2419. In addition, the mass-to-light ratio does not appear to rise towards the outer parts of the cluster. Our measurements therefore rule out the presence of a dark matter halo with mass larger than $\sim 10^7\,{\rm M}_\odot$ inside the central 500 pc, which is lower than what is found for the central dark matter densities of dSph galaxies. We also discuss the relevance of our measurements for alternative gravitational theories such as Modified Newtonian Dynamics, and for possible formation scenarios of ultracompact dwarf galaxies.

Key words: stellar dynamics – methods: *N*-body simulations – galaxies: star clusters.

1 INTRODUCTION

An important unanswered question in modern astrophysics concerns the mechanism(s) by which stars and star clusters form. This is especially true in the case of globular clusters, which, due to their large ages, are probes of the evolution and assembly history of galaxies in the early Universe.

Various theories have been proposed concerning the formation process of globular clusters. A number of authors proposed that globular clusters formed at the centres of dark matter (DM) haloes (e.g. Peebles 1984; West 1993; Cen 2001; Kravtsov & Gnedin 2005). Such a cosmologically motivated formation scenario for globular clusters is indicated by the extreme age of most clusters, their low metallicities and their characteristic masses (which are close to the Jeans mass at recombination). The fact that most clusters in the Milky Way contain no measurable amount of DM is not in contradiction to these theories, since, over the course of a Hubble time, DM would get depleted from the central regions of globular clusters due to the dynamical friction of stars against the much lighter DM particles (Baumgardt & Mieske 2008). As a result, DM tends to get pushed towards the outer cluster parts, where it is much more difficult to detect and can be more easily stripped away by the tidal field of the Milky Way (e.g. Mashchenko & Sills 2005).

A significant DM content might also be the explanation for the high mass-to-light ratios (*M*/*L*) of ultracompact dwarf galaxies (UCDs), which have been discovered in spectroscopic surveys of nearby galaxy clusters since the late 1990s (Hilker et al. 1999; Drinkwater et al. 2000). UCDs are bright ($-11 \lesssim M_V \lesssim -13.5$ mag) and compact ($7 \lesssim r_{\rm h} \lesssim 100$ pc) stellar systems that (1) appear to obey a set of structural scaling relations distinct from those of globular clusters; and (2) have *M*/*L* that are, on average, about twice as large than those of globular clusters of comparable metallicity, and somewhat larger than what one would expect based on

⋆E-mail: holger@astro.uni-bonn.de

© 2009 The Authors. Journal compilation © 2009 RAS

simple stellar evolution models assuming a standard stellar initial mass function (IMF; Haşegan et al. 2005; Dabringhausen, Hilker & Kroupa 2008; Mieske et al. 2008). One possible formation scenario for UCDs could be adiabatic gas infall into the centre of a dwarf galaxy, which also funnels DM into the centre (Goerdt et al. 2008). Later tidal disruption of these galaxies would leave only the central star cluster behind. Since some of the most massive Galactic globular clusters have masses and sizes only slightly smaller than UCDs (e.g. Rejkuba et al. 2007), it is conceivable that some of them may have formed in a similar way.

On the other hand, observations of interacting and starburst galaxies have shown that star clusters with masses comparable to globular clusters also form during major mergers between galaxies (Whitmore & Schweizer 1995; Whitmore et al. 1999; Goudfrooij et al. 2001) in the local Universe, which makes it possible that globular clusters formed by similar processes in the early Universe (e.g. Searle & Zinn 1978; Ashman & Zepf 1992). In such a scenario, globular cluster formation is driven mainly by gas-dynamical processes and the globular clusters should not contain significant amounts of DM.

Globular clusters in the outer halo of the Milky Way are ideal objects to test for the presence of DM and therefore examine the formation mechanism of globular clusters. Because the tidal field is weak in the remote halo, tidal stripping of the outer cluster regions will be much less important than for globular clusters orbiting close to the Galactic Centre. Baumgardt & Mieske (2008) have shown that, due to dynamical friction, DM gets depleted from the central regions of a star cluster on a time-scale

$$T_{\rm Fric} = 5.86 \left(\frac{M_{\rm Tot}}{10^6\,{\rm M}_\odot}\right)^{1/2} \left(\frac{r_{\rm h}}{5\,{\rm pc}}\right)^{3/2} \left(\frac{m}{{\rm M}_\odot}\right)^{-1} {\rm Gyr}, \qquad (1)$$

where $M_{\rm Tot}$ is the total cluster mass, $r_{\rm h}$ is the half-mass radius and m is the average stellar mass in the cluster. For clusters with $T_{\rm Fric} < T_{\rm Hubble}$, DM will be removed from the central parts within a Hubble time.

Fig. 1 shows the dynamical friction time-scales of Galactic globular clusters. Here the cluster masses and half-mass radii, $r_{\rm h}$, were calculated from the absolute magnitudes, projected half-mass radii $r_{\rm hp}$ and distances given by Harris (1996), assuming $M/L = 2.5$, which is appropriate for most metal-poor clusters with [Fe/H] < -1.2 and $r_{\rm h} = 1.33 r_{\rm hp}$, which is approximately correct for most King models. It can be seen that the majority of galactic globular clusters have friction time-scales much less than a Hubble time. According to the results of Baumgardt & Mieske (2008), DM would exist in such clusters only in the outer parts, where it is difficult to detect due to low stellar densities and the influence of the Galactic tidal field on the stellar velocities. Only a few clusters have friction time-scales significantly longer than a Hubble time and are therefore good candidates to look for primordial DM. Among the clusters with long dynamical friction time-scales are Pal 3, Pal 4 and Pal 14, which are currently being investigated by Haghi et al. (2009) and Jordi et al. (2009) in an effort to test alternative gravity theories like Modified Newtonian Dynamics (MOND; Milgrom 1983a,b).

The Galactic globular cluster with the longest dynamical friction time, and therefore the smallest amount of DM depletion, is NGC 2419. With a Galactocentric distance of $R_{\rm GC} \approx 90$ kpc, NGC 2419 is also one of the most remote Galactic globular clusters, meaning that tidal stripping was likely to be least effective in this cluster. Finally, NGC 2419, as one of the most massive Galactic globular clusters (see Fig. 1), represents a possible Local Group analogue to a UCD. Its half-light radius of $r_{\rm hp} = 47.5$ arcsec $\approx$ 19 pc[1] (see Section 3.1) is also ∼six times larger than is typical for globular clusters in the Milky Way and external galaxies (Jordán et al. 2005), although still a factor of ∼2 smaller than the most extreme UCDs (see e.g. table 5 of Mieske et al. 2008). For all of these reasons, NGC 2419 an excellent place to search for the presence of DM and thereby test different formation scenarios of globular clusters and, possibly, UCDs.

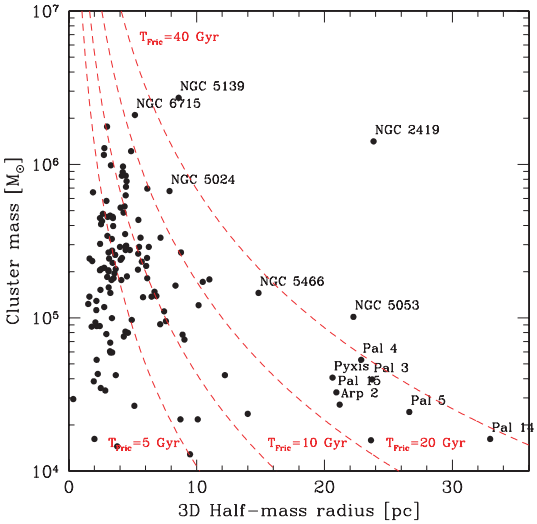

Figure 1. Dynamical friction time, $T_{\rm Fric}$, of stars against lighter DM particles for Galactic globular clusters. Most globular clusters have friction time-scales of less than a Hubble time, meaning that DM would have been depleted from their centres if they formed as a mix of DM and stars. Only a few extended clusters have friction times longer than a Hubble time and should therefore still retain DM in their centres. With the longest friction time-scale of all Galactic globular clusters, NGC 2419 is a promising target for a search for DM.

The only published velocity dispersion for NGC 2419 is that of Olszewski, Pryor & Schommer (1993) who, based on MMT radial velocity measurements with a median precision of 1.6 km s^{-1} for 12 stars, found a mean radial velocity of $v_{\rm c} = -20.0 \pm 0.9$ km s^{-1} and an intrinsic velocity dispersion of $\sigma_{\rm c} = 2.7 \pm 0.8$ km s^{-1}. Fitting single-mass, isotropic King (1962) models to their radial velocities and the cluster surface brightness profile yielded a M/L of $M/L_V \approx 0.7 \pm 0.4\,{\rm M}_\odot/L_{V,\odot}$ – one of the smallest values measured for a Galactic globular cluster and much lower than the M/L_Vs found for some UCDs.

In this paper, we report on radial velocity measurements for 44 candidate red giant branch (RGB) stars in the direction of NGC 2419 taken with the high-resolution echelle spectrometer (HIRES; Vogt et al. 1994) on the Keck I telescope. The paper is organized as follows: in Section 2 we describe the details of the observations and data reduction. In Section 3 we determine the total cluster luminosity, velocity dispersion and M/L of NGC 2419, and in Section 4 we draw our conclusions.

2 OBSERVATIONS AND DATA REDUCTION

Candidate RGB stars in NGC 2419 were selected for observation with HIRES from the photographic study of Racine & Harris (1975),

[1] At our adopted distance for NGC 2419, $(m - M)_0 = 19.60$ mag (Ripepi et al. 2007), 1 arcsec corresponds to 0.40 pc.

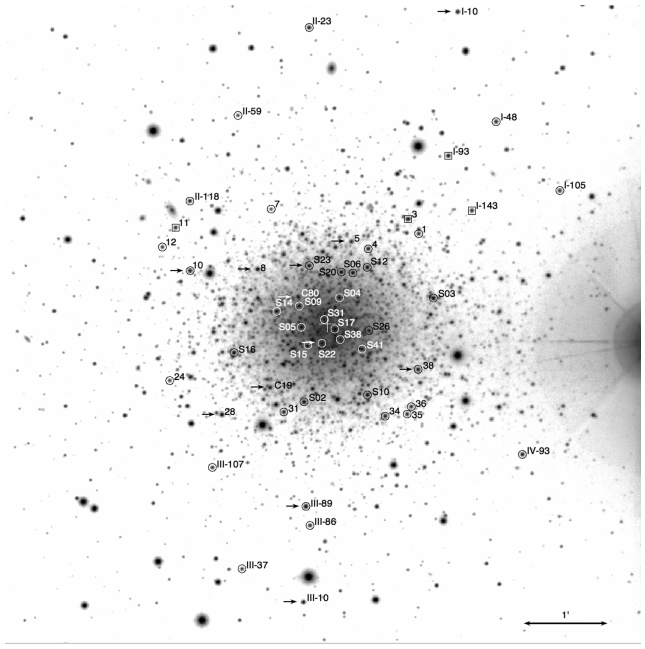

Figure 2. *V*-band finding chart for NGC 2419 showing the location of candidate RGB stars with HIRES radial velocity measurements listed in Table 1. Open circles and squares indicate cluster members and non-members, respectively. Arrows show the 12 stars with MMT radial velocity measurements from Olszewski et al. (1993). The cross shows the adopted cluster centre. North is up and east is to the left in this image, which measures $7.6 \times 7.6\,\mathrm{arcmin}^2$.

as well as from unpublished CCD photometry of Peter Stetson. Fig. 2 presents a finding chart for the candidate RGB stars that were observed for this program.

HIRES spectra were obtained on four separate nights during two observing runs on the Keck I telescope. The dates of the two runs were 1999 February 10–11 and March 9–11 (i.e. five nights in total). During each run, we limited the entrance aperture using the C1 decker ($0.866 \times 7.0\,\mathrm{arcsec}^2$) and binned the detector 1×2 (i.e. in the spatial direction) to reduce the read noise. The spectral resolution for this instrumental configuration is $\mathcal{R} = 45\,000$. A single readout amplifier was used (gain $= 2.4\,\mathrm{ADU}^{-1}$) with the red collimator and a cross-disperser in first order. Thorium–Argon comparison lamp spectra were acquired frequently during each night. In all, spectra were acquired for 44 different RGB candidates during the two runs, with exposure times ranging from 180 to 600 s. Approximately two dozen high signal-to-noise ratio (S/N) spectra for seven distinct IAU radial velocity standard stars were also obtained during the course of the program.

Spectra for program objects and standard stars were reduced in an identical manner following the general procedures described in Côté et al. (1999, 2002). Briefly, the radial velocity of each RGB candidate was measured by cross-correlating its spectrum against that of a master template created during each run from the observations of IAU standard stars. In order to minimize possible systematic effects, a master template for each observing run was derived from an identical subsample of IAU standard stars. From each cross-correlation function, we measured both v_r, the heliocentric radial velocity, and R_TD, the Tonry & Davis (1979) estimator of the strength of the cross-correlation peak.

The NGC 2419 observations discussed here were taken as part of a broader program to study the internal dynamics of outer halo globular clusters, some results of which have been reported elsewhere (i.e. Côté et al. 1999; Jordi et al. 2009). During this program, which spanned seven Keck observing runs in 1998 and 1999 (13 nights in total), we obtained 53 distinct radial velocity measurements for 23 different RGB and subgiant stars belonging to Palomar 3, Palomar 4, Palomar 5, Palomar 14 and NGC 7492, in addition to NGC 2419. Using these repeated measurements and following the procedures described in Vogt et al. (1995), we derived an empirical relationship between our radial velocity uncertainties, $\epsilon(v_\mathrm{r})$, and the strength of cross-correlation peak: $\epsilon(v_\mathrm{r}) = \alpha/(1 + R_\mathrm{TD})$, where $\alpha = 9.0^{+2.4}_{-1.6}\,\mathrm{km\,s^{-1}}$ (90 per cent confidence limits).

Our measurements are summarized in Table 1. The name of each program star is recorded in column (1), with most identifications taken directly from Racine & Harris (1975). The exception is for stars with IDs beginning with an 'S' prefix, which denotes targets selected from our (unpublished) photometric catalogue. The second column of this table gives the ID from Olszewski et al. (1993) if the star appeared in the earlier MMT study. Columns (3)–(9) record the position in right ascension (RA) and declination (Dec.), the radial distance from the cluster centre, V magnitude and $(B - V)$ colour from Stetson (2009), the number of independent HIRES radial velocity measurements and the adopted heliocentric radial velocity, v_r. For stars with multiple velocity measurements, the velocity reported in column (9) refers to the weighted mean of the individual measurements. We assumed that the cluster centre is RA (J2000) $07^\mathrm{h}38^\mathrm{m}08\overset{\mathrm{s}}{.}47$ and Dec. $+38^\circ52'56\overset{''}{.}8$ in order to calculate radial distances of stars.

In the left-hand panel of Fig. 3 we show a V, $(B - V)$ colour–magnitude diagram (CMD) for stars within 250 arcsec of NGC 2419 – extending from the tip of the RGB to the lower subgiant branch – that shows the location of our program stars in the CMD. For comparison, the solid curve shows an isochrone from Dotter et al. (2008) having $T = 12.3$ Gyr, and matching the chemical abundances of the cluster: e.g. $[\mathrm{Fe/H}] = -2.32$ dex and $[\alpha/\mathrm{Fe}] = +0.2$ dex (e.g. Shetrone, Côté & Sargent 2001). In making this comparison, we have adopted a reddening of $E(B - V) = 0.10$ mag – intermediate between the values of 0.11 and 0.08 mag reported by Harris et al. (1997) and Ripepi et al. (2007) – and a dereddened distance modulus of $(m - M)_0 = 19.60$ mag (Ripepi et al. 2007). Note that all of our program stars, and those from the previous MMT program, are located within ∼2 mag of the RGB tip. The right-hand panel of Fig. 3 shows a magnified view of this part of the CMD. The dashed lines show a region of ±0.15 mag width centred on the isochrone – an interval chosen to roughly match the observed width of the RBG sequence and encompass all of the probable radial velocity members.

Since NGC 2419 is located at a Galactic latitude of $b \simeq 25^\circ$, it is important to consider the possibility of contamination by foreground disc stars. To gauge the extent of such contamination, we show in the right-hand panel of Fig. 3 the results of one simulation using the Besançon Galaxy model (Robin et al. 2003), for field stars in the range 0–100 kpc and located within a $500 \times 500\,\mathrm{arcsec}^2$ region in the direction of NGC 2419. This simulation yields a total of 10 stars having magnitudes and colours that would place them within the region bounded by the dashed lines in the right-hand panel of Fig. 3. However, as we shall see in Section 3.2, only two stars in this simulation have radial velocities within $\pm 3\sigma$ of the cluster mean. Since our radial velocity survey is by no means complete within this simulated region, we conclude that our final sample should have minimal foreground contamination with one interloper, *at most*, expected within $\pm 3\sigma$ of the cluster's systemic velocity. The final column of Table 1 gives our division of the sample into cluster members and foreground stars. In most cases, the assignments are

Table 1. Radial velocities for candidate red giants in NGC 2419.

ID	093	RA (J2000.0)	Dec. (J2000.0)	R (arcsec)	V (mag)	$(B-V)$ (mag)	N_{v_r}	v_r (km s^{-1})	Member?
(1)	(2)	(3)	(4)	(5)	(6)	(7)	(8)	(9)	(10)
III89	III89	07 38 09.79	+38 50 45.4	132.3	17.25	1.42	1	-26.05 ± 0.92	Y
S3	.....	07 38 01.92	+38 53 15.4	78.7	17.26	1.44	1	-26.52 ± 0.61	Y
S2	.....	07 38 09.90	+38 52 00.7	58.5	17.27	1.55	1	-15.56 ± 0.53	Y
S4	.....	07 38 07.71	+38 53 15.7	20.9	17.27	1.51	1	-24.27 ± 0.66	Y
S5	.....	07 38 10.07	+38 52 54.3	18.9	17.29	1.48	1	-16.41 ± 0.67	Y
S12	.....	07 38 06.00	+38 53 37.5	49.9	17.40	1.39	1	-22.16 ± 0.63	Y
S6	.....	07 38 06.89	+38 53 33.5	41.1	17.41	1.28	1	-16.24 ± 0.71	Y
S14	.....	07 38 11.58	+38 53 05.8	37.4	17.42	1.32	1	-12.22 ± 0.61	Y
S9	.....	07 38 10.18	+38 53 09.6	23.7	17.42	1.24	1	-15.95 ± 0.56	Y
34	.....	07 38 04.90	+38 51 50.6	78.2	17.43	1.35	1	-20.96 ± 1.28	Y
S10	.....	07 38 16.92	+38 53 35.0	105.8	17.43	1.35	1	-20.75 ± 0.58	Y
S17	.....	07 38 08.01	+38 52 53.1	6.5	17.46	1.22	1	-10.12 ± 0.81	Y:
S15	.....	07 38 09.69	+38 52 40.9	21.4	17.48	1.43	1	-16.79 ± 0.58	Y
S20	.....	07 38 07.60	+38 53 34.1	38.7	17.50	1.38	1	-23.66 ± 0.55	Y
S16	.....	07 38 14.21	+38 52 36.0	70.2	17.51	1.36	1	-19.99 ± 0.46	Y
S22	C37	07 38 08.80	+38 52 42.9	14.4	17.51	1.31	1	-33.98 ± 0.64	Y:
S23	C80	07 38 09.57	+38 53 38.7	43.8	17.54	1.32	1	-22.81 ± 0.58	Y
S26	.....	07 38 05.90	+38 52 52.0	30.4	17.57	1.38	1	-27.17 ± 0.53	Y
10	10	07 38 16.92	+38 53 35.0	105.8	17.61	1.28	2	-19.58 ± 0.56	Y
38	.....	07 38 02.87	+38 52 24.1	73.1	17.61	1.41	3	-23.63 ± 0.40	Y
3	.....	07 38 03.48	+38 54 12.1	95.2	17.63	1.34	1	20.76 ± 0.79	N
S31	.....	07 38 08.64	+38 53 00.0	3.8	17.64	1.19	1	-23.69 ± 0.43	Y
S38	38	07 38 07.67	+38 52 45.5	14.7	17.75	1.18	1	-10.22 ± 0.43	Y:
S41	.....	07 38 06.32	+38 52 38.7	31.0	17.79	1.27	1	-29.27 ± 0.44	Y
IV93	.....	07 37 56.45	+38 51 22.8	169.0	17.80	1.29	1	-20.64 ± 0.69	Y
II23	.....	07 38 09.58	+38 56 30.0	213.6	17.95	1.14	1	-20.67 ± 0.89	Y
4	.....	07 38 05.94	+38 53 50.8	61.6	17.97	1.27	2	-23.49 ± 0.83	Y
31	.....	07 38 11.15	+38 51 53.4	70.7	18.07	1.17	1	-18.02 ± 1.08	Y
I93	.....	07 38 01.00	+38 54 57.8	149.1	18.08	1.54	1	70.61 ± 0.99	N
II118	.....	07 38 16.93	+38 54 25.2	132.5	18.09	1.15	1	-20.75 ± 1.04	Y
I48	.....	07 37 58.06	+38 55 22.2	189.5	18.13	1.12	2	-18.47 ± 0.71	Y
I105	.....	07 37 54.13	+38 54 32.7	192.9	18.16	1.16	1	-21.43 ± 0.97	Y
III86	.....	07 38 09.54	+38 50 31.7	145.6	18.23	1.19	1	-18.89 ± 0.99	Y
11	.....	07 38 17.81	+38 54 06.1	129.2	18.23	1.10	1	48.83 ± 0.64	N
III37	.....	07 38 13.72	+38 50 00.5	186.7	18.29	1.05	1	-21.30 ± 1.20	Y
36	.....	07 38 03.29	+38 51 57.2	84.9	18.31	1.23	1	-20.90 ± 1.29	Y
35	.....	07 38 03.55	+38 51 51.9	86.7	18.32	1.18	1	-18.45 ± 0.98	Y
III107	.....	07 38 15.55	+38 51 13.5	132.3	18.39	1.06	1	-17.43 ± 0.99	Y
I143	.....	07 37 59.55	+38 54 18.2	132.2	18.39	1.39	1	45.81 ± 0.62	N
12	.....	07 38 18.63	+38 53 52.0	130.8	18.60	1.02	1	-17.70 ± 1.16	Y
1	.....	07 38 02.83	+38 54 01.7	92.5	18.61	1.01	1	-21.63 ± 1.31	Y
24	.....	07 38 18.18	+38 52 15.9	120.5	18.70	0.98	1	-21.68 ± 1.11	Y
II59	.....	07 38 13.97	+38 55 26.7	163.1	18.80	0.98	1	-23.20 ± 1.11	Y
7	.....	07 38 11.93	+38 54 19.4	92.0	19.00	0.95	1	-22.40 ± 1.26	Y

unambiguous, although three stars (S17, S22 and S38) are more problematical. We shall return to this issue in Section 3.

3 RESULTS

3.1 Surface density profile

The surface brightness profile of NGC 2419 has most recently been determined by Bellazzini (2007) using surface photometry and star counts from *Hubble Space Telescope*/Advanced Camera for Surveys (*HST*/ACS) and Sloan Digital Sky Survey (SDSS). In this paper we use his data for our analysis. Fig. 4 shows the V-band surface brightness profile of NGC 2419 as determined by Bellazzini (2007) and compares it with several different model profiles. Bellazzini (2007) found that the best-fitting King (1962) profile has a central core radius of $r_c = 19.2$ arcsec and a concentration index of $c = \log(r_t/r_c) = 1.35$. We show this profile by the blue dashed curve in Fig. 4. As can be seen, a King profile provides a satisfactory fit to the observed surface density profile out to ≈300 arcsec. Beyond this point, however, the observed brightness profile declines more slowly than the fitted King profile. Such an excess could be the signature of extratidal stars (e.g. Leon, Meylan & Combes 2000). However, at the distance of NGC 2419, 300 arcsec corresponds to a physical distance of about 120 pc. The expected tidal radius of NGC 2419 at its current distance is $r_t \sim 750$ pc: i.e. more than five times as large, if we assume a circular cluster orbit and a logarithmic potential with circular velocity $v_c = 200\,\mathrm{km\,s^{-1}}$ for the Milky Way and a cluster mass of $10^6\,M_\odot$. In addition, tidal radii often correspond to breaks in the surface density distribution but no such break is visible in Fig. 4. Hence, unless the cluster orbit is highly eccentric ($\epsilon > 0.9$),

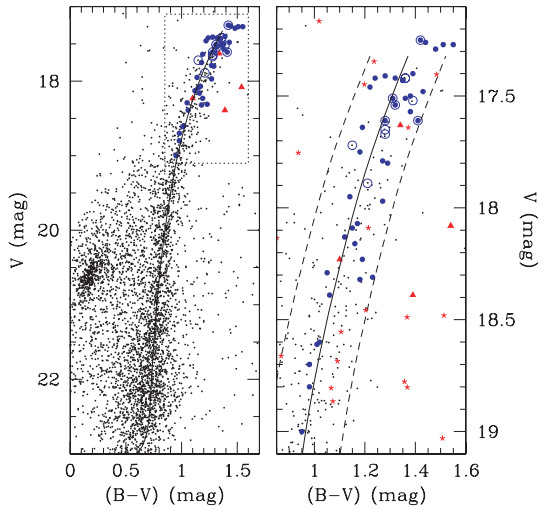

Figure 3. Left-hand panel: CMD for NGC ∼ 2419 from our own unpublished photometry, showing the location of our program stars. Filled blue circles show the 40 probable members according to our HIRES radial velocities. Open circles show the 12 stars with radial velocities measurements from Olszewski et al. (1993); there are five stars in common between the two studies. Red triangles show the four obvious non-members stars from Table 1. The smooth curve shows a 12.3-Gyr isochrone (Dotter et al. 2008) with [Fe/H] = −2.32 dex and [α/Fe] = +0.2 dex, shifted by $E(B-V) = 0.10$ mag and $(m-M)_V = (m-M)_0 + A_V = 19.91$ mag to match the RGB. Right-hand panel: magnified view of the dotted region from the previous panel. The dashed curves show a ±0.15-mag region centred on the isochrone. The red asterisks illustrate one simulation of the expected contamination in region of the CMD from Galactic foreground stars in the direction of NGC 2419 using the Besançon Galaxy model (Robin et al. 2003). See text for details.

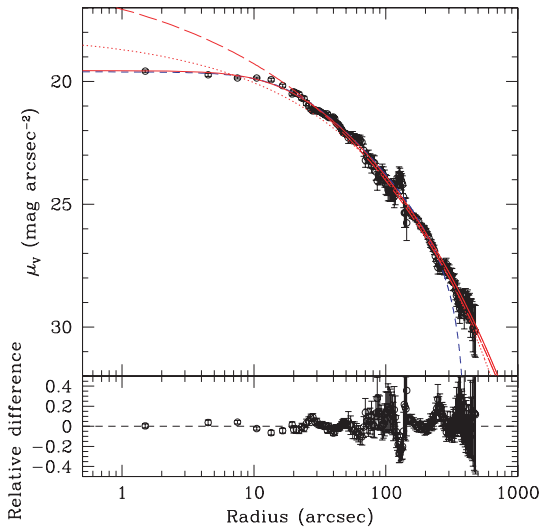

Figure 4. Upper panel: *V*-band surface brightness profile of NGC 2419 as determined by Bellazzini (2007). The blue, short-dashed curve shows the best-fitting single-mass, isotropic King model. This model cannot fit the 'excess' light at large radii. The dotted and long-dashed red curves are fits of two Sérsic profiles that fit the outer parts of the cluster well but not the central region. The solid curve is a Sérsic profile with an added core of size $r_c = 14$ arcsec. It provides a good match to the density profile and is within the reported observational uncertainties at most radii (bottom panel).

the outermost stars are most likely bound to NGC 2419 so that the tidal radius has not yet been reached by the observations, something which was also noted by Ripepi et al. (2007).

We have therefore also tried to fit the surface brightness profile with Sérsic (1963) profiles, which are known to provide accurate representations of the surface brightness profiles of most early-type galaxies, including UCDs, over nearly their entire profiles (e.g. Graham & Guzmán 2003; Ferrarese et al. 2006; Côté et al. 2007; Evstigneeva et al. 2007; Hilker et al. 2007). We find that Sérsic models that best fit the data over the whole range (red dotted curve) and those fitted to the data for $r > 20$ arcsec both give good fits in the outer profiles but significantly overpredict the central surface brightness. In order to obtain a model that fits the surface brightness profile over the whole radial range, we add a constant density core to the Sérsic profile fitted to the data for $r > 20$ arcsec:

$$\Sigma(r) = \Sigma_0 \exp[-(1.9992n - 0.3271)(r'/r_e)^{1/n} - 1.0], \quad (2)$$

where $r' = \sqrt{r^2 + r_c^2}$. A χ^2 minimization gives 14 arcsec as best-fitting value for r_c. The solid red curve in Fig. 4 shows the surface brightness profile of the outer Sérsic profile once a constant density core with $r_c = 14$ arcsec has been added. With this model we obtain a very good fit to the overall surface brightness profile. The lower panel shows the residuals between our fitted model and the observed data. At most radii, the differences between the observed surface density and our model are within the observational uncertainties.

Table 2 summarizes our results. For a King model fit, we find that the best-fitting profile has $r_c = 19$ arcsec and $c = 1.39$, which agrees reasonably well with Bellazzini (2007). The other rows list the parameters of our best-fitting Sérsic profiles. The integrated *V* magnitudes are calculated separately for each surface density profile. They are, in general, somewhat smaller than the values by Bellazzini (2007), who found $V = 10.47 \pm 0.07$ mag. Because the King profile underpredicts the light in the outer parts while the two Sérsic profiles significantly overpredict the light in the inner parts, we consider the values from the cored Sérsic profile to be most reliable and we will use them in the remainder of this paper. For the cored Sérsic profile, we obtain a total luminosity of $V = 10.57$ mag and a projected half-light radius of $r_{hp} = 47.5$ arcsec. The latter value agrees quite well with the half-light radius found by Trager, King & Djorgovski (1995), $r_{hp} = 45.7$ arcsec. With a distance modulus of $(m-M)_0 = 19.60 \pm 0.05$ mag and a reddening of $E(B-V) = 0.08$ mag (Ripepi et al. 2007), these values lead to a total absolute magnitude and projected half-mass radius of NGC 2419 of $M_V = -9.28$ mag and $r_{hp} = 19.2$ pc, respectively.

3.2 Velocity dispersion of NGC 2419

Table 1 lists 44 stars in the direction of NGC 2419 with radial velocities measured in the course of this study. Rejecting the four stars

Table 2. Photometric parameters of best-fitting surface density profiles for NGC 2419.

	c	r_c (arcsec)	r_{hp} (arcsec)	μ_0 (mag arcsec^{-2})	V_{tot} (mag)
King model	1.39	19.0	44.7	19.61	10.65
	n	r_e (arcsec)	r_{hp} (arcsec)	μ_e (mag arcsec^{-2})	V_{tot} (mag)
Sérsic (all *r*)	2.15	49.8	49.8	22.32	10.77
Sérsic ($r > 20$ arcsec)	3.01	33.2	33.2	21.31	10.48
Sérsic-core	3.01	33.2	47.5	21.23	10.57

© 2009 The Authors. Journal compilation © 2009 RAS, MNRAS **396,** 2051–2060

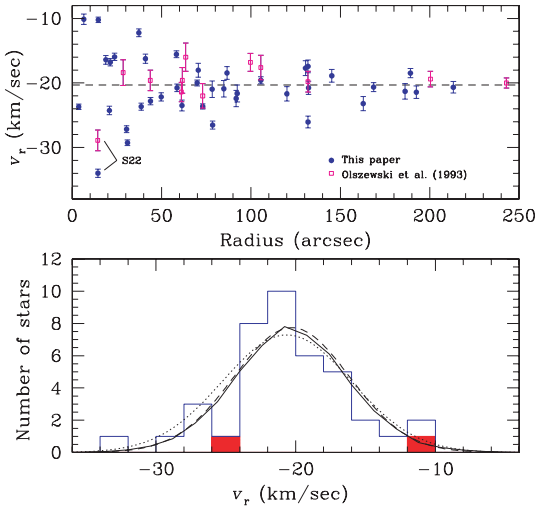

Figure 5. Upper panel: heliocentric radial velocity for NGC 2419 probable members plotted as a function of distance from the cluster centre. The dashed line shows our best estimate for the cluster systemic velocity, $\langle v_r \rangle \approx -20.3\,\mathrm{km\,s^{-1}}$. There is a clear rise in velocity dispersion toward the cluster centre. Note the discrepant measurements for star S22, which is the largest outlier in both our sample and that of Olszewski et al. (1993). Lower panel: radial velocity distribution of the measured stars in NGC 2419. Dotted and dashed lines show Gaussian fits to this distribution obtained by either using all stars from Table 1 (dotted line), or by excluding star S22 – which has the most discrepant velocity – from the sample (dashed line). The filled red histogram shows the expected distribution, in this velocity interval, for foreground stars within a $500 \times 500\,\mathrm{arcsec^2}$ region along this line of sight and falling along the RGB in the cluster CMD (see the right-hand panel of Fig. 3). The solid line shows the distribution of stars from our model cluster fitted to the data without star S22. It follows very closely the corresponding Gaussian distribution (dashed line).

with the most discrepant velocities and consequently identified as non-members in Table 1 (e.g. S3, I93, 11 and I143) leaves us with a sample of 40 stars having radial velocities in the range $-35 \leq v_r \leq -5\,\mathrm{km\,s^{-1}}$. Although this sample shows a clear peak at $\sim -20\,\mathrm{km\,s^{-1}}$ corresponding to the cluster systemic velocity, there are three stars that differ by $\sim$10 km s^{-1} or more from the apparent cluster mean. The upper panel of Fig. 5, which plots radial velocity against distance from the cluster centre, reveals all three to be among the centrally concentrated stars (i.e. with radii of $r \lesssim 15$ arcsec) and thus unlikely to be interlopers. Nevertheless, we now pause to consider the extent to which our sample could be contaminated by foreground disc stars.

As noted in Section 2, one simulation of the expected Galactic foreground using the Besançon model (Robin et al. 2003) suggests we might expect *a total* of $\sim$10 interloping field stars: (1) within a $500 \times 500\,\mathrm{arcsec^2}$ region along this line of sight; and (2) falling along the cluster RGB shown in the right-hand panel of Fig. 3. In the lower panel of Fig. 5 we compare the observed velocity distribution of radial velocities (open blue histogram) with that from the simulation (filled red histogram). The foreground stars plotted here represent all stars in this velocity range with magnitudes and colours that place them within the RGB locus shown in Fig. 3. Because our sample of 44 RGB candidates constitutes only a small fraction ($\approx$13 per cent) of the full sample of stars in this region of the CMD and lying within $\sim$250 arcsec of the cluster core, we conclude that we would expect, at most, one interloper in our final sample of 40 cluster members.

We now proceed by calculating the average radial velocity and velocity dispersion of NGC 2419 using the method of Pryor & Meylan (1993). We first assume that each velocity, v_i, is drawn from a normal distribution:

$$f(v_i) = \frac{1}{\sqrt{2\pi\left(\sigma_c^2 + \sigma_{e,i}^2\right)}} \exp\left[-\frac{(v_i - v_c)^2}{2\left(\sigma_c^2 + \sigma_{e,i}^2\right)}\right], \quad (3)$$

where v_c and σ_c are the cluster's average radial velocity and intrinsic velocity dispersion, and $\sigma_{e,i}$ is the individual velocity error for each star. Calculating the likelihood function, L, for all stars and taking the partial derivatives of its logarithm $l = \log L$ with respect to v_c and σ_c leads to the following set of equations:

$$\sum_{i=1}^{N} \frac{v_i}{\left(\sigma_c^2 + \sigma_{e,i}^2\right)} - v_c \sum_{i=1}^{N} \frac{1}{\left(\sigma_c^2 + \sigma_{e,i}^2\right)} = 0, \quad (4)$$

$$\sum_{i=1}^{N} \frac{(v_i - v_c)^2}{\left(\sigma_c^2 + \sigma_{e,i}^2\right)^2} - \sum_{i=1}^{N} \frac{1}{\left(\sigma_c^2 + \sigma_{e,i}^2\right)} = 0. \quad (5)$$

The above equations can be solved analytically to obtain a first guess value for v_c and σ_c if zero measurement errors $\sigma_{e,i}$ for all stars are assumed. The full solution can then be obtained iteratively, starting with the solution for zero measurement errors as first estimate. The errors of v_c and σ_c are obtained from the information matrix, I, by

$$\sigma_v = I_{22} / \left(I_{11} I_{22} - I_{12}^2\right), \quad (6)$$

$$\sigma_\sigma = I_{11} / \left(I_{11} I_{22} - I_{12}^2\right), \quad (7)$$

where the components I_{ij} of the information matrix are calculated as given in Pryor & Meylan (1993).

Using the 40 probable members from Table 1, we obtain a mean cluster velocity of $v_c = -20.63 \pm 0.74\,\mathrm{km\,s^{-1}}$ and an intrinsic velocity dispersion of $\sigma_c = 4.61 \pm 0.53\,\mathrm{km\,s^{-1}}$. This mean velocity agrees very well with the one obtained by Olszewski et al. (1993). Our velocity dispersion is, however, significantly higher than the value of $2.7 \pm 0.8\,\mathrm{km\,s^{-1}}$ determined by Olszewski et al. (1993) and agrees with their value only at the 2σ level. The explanation for this difference appears to lie in the radial distribution of the stars in the two samples: Fig. 5 reveals the Olszewski et al. (1993) sample to contain only three stars in the central $r \sim 1$ arcmin, where we observe a significant rise in the cluster velocity dispersion based on a larger sample of 17 stars in this region. In the outer parts of the cluster, our measured velocity dispersion (see below) is in very good agreement with the previous estimate.

The lower panel of Fig. 5 shows the distribution of radial velocities of the 40 candidate members in the velocity range -36 to $-4\,\mathrm{km\,s^{-1}}$ (open histogram). The dotted curve shows a Gaussian fit to this distribution using the above values for v_c and σ_c. As can be seen, the observed radial velocity distribution is well approximated by this Gaussian except, as noted above, that the number of outliers in the wings of the distribution is somewhat higher than predicted: i.e. stars S17 and S38 are more than 2.2σ away from the mean while star S22 is almost 3σ away from the mean. For a Gaussian distribution and a sample of 40 stars, one would expect to find a star that is more than 3σ away from the mean in only 10 per cent of all cases. Furthermore, the chance to have three or more stars more than 2.2σ away from the mean is only 10 per cent, while the chance to have two such stars is twice has high. This makes it possible that at least one star, most likely star S22, is either a cluster non-member or a radial velocity variable.

Since star S22 is located in the cluster centre and has a photometry that places it squarely on the RGB (see the right-hand panel

of Fig. 3), it could be a binary system, in which case it should be excluded from the analysis. The absolute radial velocity difference between star S22 and the cluster mean ($\sim$15 km s^{-1}) is also so large that star S22 would be nearly unbound if the radial velocity difference is due to a different orbital velocity. Star S22 is also one of the five stars in common with Olszewski et al. (1993), and has the most discrepant velocity in both samples. Moreover, two independent measurements different by 5.1 km s^{-1}, or three times the quadrature sum of the individual uncertainties. These facts suggest that star S22 may be a cluster binary or, perhaps more likely, an RGB star that shows a velocity 'jitter' that has previously been found for some globular cluster stars on the upper RGB (e.g. Gunn & Griffin 1979; Mayor et al. 1984). If we omit star S22, we obtain a mean cluster velocity and an intrinsic velocity dispersion of

$$v_{\rm c} = -20.28 \pm 0.68 \ {\rm km\,s^{-1}},$$
$$\sigma_{\rm c} = 4.14 \pm 0.48 \ {\rm km\,s^{-1}}. \quad (8)$$

These values are within the error bars of the values that we obtain when using all stars and we will use them throughout the rest of this paper.

We note that the three stars with the most discrepant radial velocities are also among the four most central stars. While this could simply be a statistical effect, it could also point to either a high binary fraction in the core or the broadening of the velocity distribution due to additional unseen mass, possible if the cluster is mass segregated or contains an intermediate-mass black hole (Baumgardt, Makino & Hut 2005). Multi-epoch observations of the stars in our sample and radial velocities of additional core stars would be required to test these interesting possibilities.

3.3 Cluster rotation

Our sample of 40 member stars also allows us to check for a possible rotation of NGC 2419. Fig. 6 shows the radial velocities of stars as a function of position angle (PA). Here the PA is measured from north (PA = 0°) towards east (PA = +90°). There is a clear dependence of the average velocity from the PA visible in the data. This is confirmed by fitting a sinusoidal curve to the radial velocity data. Allowing for a variable rotation angle, we obtain a rotation amplitude of 3.26 ± 0.85 km s^{-1} around an axis with PA = $40\overset{\circ}{.}9 \pm 17\overset{\circ}{.}8$. Our data therefore implies cluster rotation at more than the 3σ level. The root mean square scatter around the rotation curve is 4.00 km s^{-1}. NGC 2419 is therefore partly rotationally supported and partly supported by random stellar motions. Bellazzini (2007) found that NGC 2419 is slightly elliptical with average ellipticity of $\epsilon = 0.19 \pm 0.15$ and PA = $+105^\circ \pm 28^\circ$. Both the relatively small amount of ellipticity and the average angle of ellipticity, which is within the error bars 90° away from the rotation axis that we find, supports our finding that NGC 2419 is rotating.

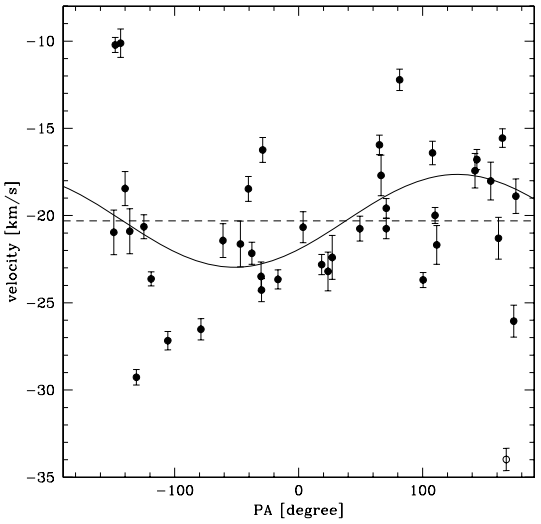

Figure 6. Radial velocities as a function of PA measured from north (PA = 0°) towards east. The solid curve shows our best-fitting rotation curve for NGC 2419. It has an amplitude of 3.26 ± 0.85 km s^{-1}, implying significant rotation of the cluster. The direction of rotation, PA = $40\overset{\circ}{.}9 \pm 17\overset{\circ}{.}8$ is, within the error bars 90° away from the semimajor axis found in the surface density profile by Bellazzini (2007), PA = $+105^\circ \pm 28^\circ$, supporting the fact that NGC 2419 is rotating.

3.4 Mass modelling and mass-to-light ratio

The global M/L is calculated from the velocity dispersion and the total cluster luminosity under the assumption that mass follows light. Unless there is primordial mass segregation, this is probably a valid assumption since the relaxation time of NGC 2419 is larger than a Hubble time, i.e. the central and half-mass relaxation times are $T_{\rm r0} \approx 10.5$ Gyr and $T_{\rm rh} \approx 19$ Gyr, respectively (Djorgovski 1993). In addition, Dalessandro et al. (2008) found no evidence for mass segregation among the blue straggler stars in NGC 2419, which supports the assumption that mass follows light. We also neglect the cluster rotation and assume that the cluster has an isotropic velocity dispersion. In such a case, we can use the method described in Hilker et al. (2007) to calculate the M/L. Their method first deprojects the surface density profile (here a cored Sérsic profile) to obtain the three-dimensional spatial density distribution, $\rho(r)$. The spatial density is then used to calculate the potential, $\Phi(r)$, of NGC 2419 and from ρ and Φ, the distribution function, $f(E)$, is calculated by assuming spherical symmetry and using equation (4-140a) of Binney & Tremaine (1987). This distribution function is then used to create an N-body representation (i.e. particle positions and velocities) of NGC 2419 with a given first guess of M' for the cluster mass. We then draw a number of N' stars located at the same projected radius of each observed star from this N-body model and measure the projected velocity dispersion, $\sigma_{\rm Mod}$, of the sample stars. The total mass of NGC 2419 can then be calculated by comparing this velocity dispersion with the observed velocity dispersion according to

$$M_{\rm C} = M' \, \sigma^2_{\rm Mod} \Big/ \sigma^2_{\rm c}. \quad (9)$$

This method has the advantage that it can work for any given observed surface density profile and for any given radial distribution of stars. This sets it apart from parametrized formulas which work only for certain density distributions and usually need the core or global velocity dispersion to calculate the cluster mass. If the stars with radial velocity measurements are neither concentrated in the cluster core nor spread out over the cluster in the same way as the cluster stars, using such formulae can lead to a bias in the derived cluster mass.

We calculate an N-body model with $N = 5 \times 10^5$ stars in total and extract for each observed star $N' = 200$ stars from this model. Calculating the velocity dispersion for the theoretical model and comparing it with NGC 2419, we find a total mass of $M_{\rm C} = (9.02 \pm 2.22) \times 10^5 \, {\rm M}_\odot$ for NGC 2419 and a M/L of $M/L_V = 2.05 \pm 0.50$ in solar units, using all stars except star S22. If we were to include star S22, the total mass would rise to $M_{\rm C} = (1.09 \pm 0.26) \times 10^6 \, {\rm M}_\odot$ and the M/L would be $M/L_V = 2.48 \pm 0.60$ in solar units. These values are significantly higher than the M/L ratio

© 2009 The Authors. Journal compilation © 2009 RAS, MNRAS **396,** 2051–2060

derived by Olszewski et al. (1993), $M/L_V \approx 0.7 \pm 0.4\,M_\odot/L_{V,\odot}$. Since our method gives a very similar M/L than what they found if we use their stars as input, the main reason for the discrepant M/L values seems to be the different input stars.

We finally tested our modelling method by randomly drawing 40 stars from the N-body model and then measuring their velocity dispersion and fitting the model against them in the same way as was done for the NGC 2419 data. Doing this 100 times, each time with a different random realization of stars, we obtained an average ratio of derived M/L to true M/L of 1.00 ± 0.01, i.e. our modelling method gives an unbiased estimate of the true M/L.

In order to compare the observed M/L with the predictions of population synthesis models, we need to know the cluster age and metallicity. Based on an analysis of a high-resolution Echelle spectrum for a single RGB star (10), Shetrone et al. (2001) measured a metallicity of [Fe/H] $= -2.32$ for NGC 2419, which is one of the lowest abundances among all Galactic globular clusters. Salaris & Weiss (2002) have used horizontal branch and turn off star brightnesses to determine ages of Galactic globular clusters and derived an absolute age of 12.3 or 12.8 Gyr for NGC 2419, depending on the adopted metallicity scale. For this metallicity and age, the SSP models of Maraston (2005) predict a M/L of 1.95 for a Kroupa (2001) IMF, while the Bruzual & Charlot (2003) models predict $M/L_V = 1.85$ for a Chabrier (2003) IMF. These values agree remarkably well with the derived M/L. The M/L_V ratio of NGC 2419 is therefore entirely compatible with the assumption that the cluster formed with a standard stellar mass function. This sets NGC 2419 apart from some UCDs, which have only slightly larger sizes and masses, and for which standard mass functions seem to underpredict their M/Ls (Haşegan et al. 2005; Mieske et al. 2008).

The 'normal' M/L of NGC 2419 also argues against the presence of a significant amount of DM in the cluster. In order to test if a possible DM halo could exist at least in the outer cluster parts, we have divided the sample into three equally large groups according to their radial distance and calculated velocity dispersions separately for each group. Fig. 7 compares velocity dispersions at different radii with the predicted velocity dispersion profile from our N-body model. It can be seen that the velocity dispersion of the cored Sérsic model is in reasonable agreement with the data. If at all, additional mass is required only in the inner parts of the cluster, where the predicted velocity dispersion is smaller than the observed one by about 1σ, not in the outer parts as might be expected for a DM halo.

We also added different DM haloes to our N-body model in order to see the effect of these haloes on the velocity dispersion. The DM haloes follow NFW profiles with scale radii $R_S = 500$ pc, which agrees with measured scale radii of Galactic dSph galaxies which are generally larger than a few hundred pc (Wu 2007), and had various ratios of dark halo mass inside R_S to the stellar mass of NGC 2419. We then calculated a new velocity dispersion profile for NGC 2419 and fitted it to the data in the same way as described above. From our fit procedure, we derive a best-fitting (stellar) M/L ratio and the total stellar and dark mass of NGC 2419. As can be seen in Fig. 7, significant amounts of DM are basically ruled out by our observations since they overpredict the velocity dispersion in the outer cluster parts, at least for models with isotropic stellar velocity dispersions. A DM halo with total mass of $M_{\rm DM} = 1.65\,M_{\rm Stars}$ overpredicts the velocity dispersion by more than 2σ at a radius of $R = 140$ arcsec. This model also has a best-fitting stellar M/L ratio of only $M/L = 1.40 \pm 0.34$, which is 2σ below the predictions of the stellar evolution models. Our observations therefore rule out a DM halo of more than $M \approx 1 \times 10^7\,M_\odot$ inside 500 pc around NGC 2419, corresponding to a density of $0.02\,M_\odot\,{\rm pc}^{-3}$.

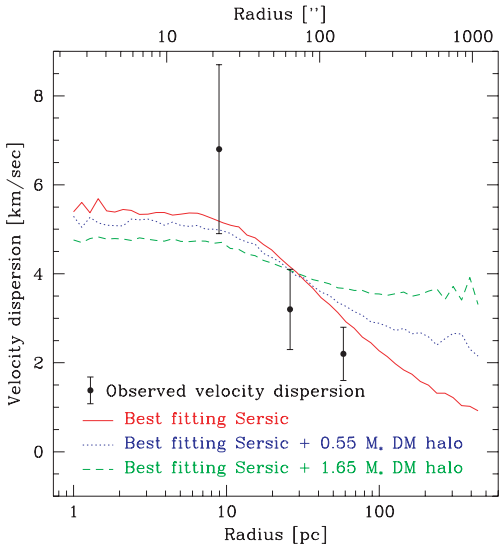

Figure 7. Observed velocity dispersion as a function of radius. The solid line shows our prediction based on the best-fitting cored Sérsic model. Dotted and dashed lines show the predicted velocity dispersion if we add NFW haloes with a scale radius of $R_S = 500$ pc and masses of $M_{\rm DM} = 4 \times 10^6$ and $10^7\,M_\odot$ inside R_S to this model. Models with additional DM haloes significantly overpredict the velocity dispersion in the outer parts, showing that NGC 2419 does not possess a dSph-like DM halo.

This is significantly lower than the DM content of Galactic dSph galaxies inside a similar radius as derived by Walker et al. (2007) and Strigari et al. (2008). It is also a factor of 5 lower than central DM densities of dwarf galaxies as determined by Gilmore et al. (2007). Our observations therefore argue strongly against the formation of NGC 2419 within a sizeable DM halo. More radial velocities would help to strengthen our conclusions and test the validity of several assumptions that we made for our data analysis, in particular that the stellar orbits are isotropic and that the cluster is not mass segregated.

Finally, we note that the low observed velocity dispersion in the outer parts of NGC 2419 might also be a problem for MOND. According to MOND, the orbits of stars show a difference with respect to standard Newtonian behaviour once their acceleration falls below a critical acceleration $a_0 \sim 1.2 \times 10^{-8}\,{\rm cm\,s^{-2}}$ (Sanders & McGaugh 2002). While the acceleration of stars near the half-mass radius of NGC 2419 is still higher than a_0, it falls significantly below a_0 in the outer parts of NGC 2419. At the radius of our outermost data point in Fig. 7, the internal acceleration is only one third of a_0, while the external acceleration is only one tenth of a_0, so one would expect that the observed velocities start to deviate significantly from the prediction of our N-body model which was created based on Newtonian dynamics. This is not seen in our data. In fact, as shown by Milgrom (1994), if one neglects the external field of the Milky Way, MOND predicts that the line-of-sight velocity dispersion should level off at a value $\sigma_{\rm min} = 0.471\sqrt{G M_C/a_0}$ at large distances. If we use the above calculated cluster mass, we find $\sigma_{\rm min} = 2.6\,{\rm km\,s^{-1}}$ for NGC 2419. Our outermost data point is already probing this value, so acquiring additional data at even larger radii might prove a powerful way to test the validity of MOND.

4 CONCLUSIONS

We have measured precise radial velocities for ≈40 stars in the outer halo globular cluster NGC 2419 using the Keck telescope High Resolution Echelle Spectrometer. We find a mean cluster velocity of

$\langle v_r \rangle = -20.3 \pm 0.7\,\mathrm{km\,s^{-1}}$ and an internal velocity dispersion of $\sigma = 4.14 \pm 0.48\,\mathrm{km\,s^{-1}}$. Our observations also reveal a slight cluster rotation with amplitude $3.26 \pm 0.85\,\mathrm{km\,s^{-1}}$ around a PA of $40.^{\circ}9 \pm 17.^{\circ}8$. From a comparison of the measured velocity dispersion to the velocity dispersion of an spherically symmetric model for NGC 2419, we find a total mass of $M_C = (9.01 \pm 2.22) \times 10^5\,M_\odot$ and a M/L of $M/L_V = 2.05 \pm 0.50$ in solar units. This value is entirely compatible with the one expected for a stellar system at the metallicity of NGC 2419 following a standard mass function like Kroupa (2001) or Chabrier (2003).

NGC 2419 therefore does not show any dynamical evidence of a significant depletion of low-mass stars, which is consistent with expectations given the large relaxation and dissolution time for this cluster. Similar M/L ratios which are in agreement with standard mass functions have been found for other galactic globular clusters with large relaxation and dissolution times like ω Cen ($M/L_V = 2.5$; van de Ven et al. 2006). This sets Milky Way globular clusters apart from UCDs for which standard mass functions on average seem to underpredict M/Ls (Mieske et al. 2008). If real, this points to a significant change in the star formation process occurring at a characteristic mass of $M_C \approx 2 \times 10^6\,M_\odot$ (e.g. Haşegan et al. 2005; Mieske et al. 2008; Dabringhausen, Kroupa & Baumgardt 2009). Such a transition might arise, for example, if more massive clusters become optically thick to far-infrared radiation and are born with top heavy IMFs (Murray 2009).

We do not find any evidence for the presence of substantial amounts of DM in NGC 2419. Since both the depletion of DM from the cluster centre due to two-body relaxation and dynamical friction (Baumgardt & Mieske 2008), as well as tidal stripping of DM from the cluster halo are unlikely, this indicates that NGC 2419 did not contain substantial amounts of DM at the time of formation. NGC 2419 is, however, one of the most likely candidates for a globular cluster to have formed with an associated DM halo given to its quite low metallicity. Our non-detection of DM in this cluster therefore supports the hypothesis that globular clusters, as a rule, did not form at the centres of DM haloes. Instead, an origin driven by gas dynamical processes during mergers between galaxies (Bournard, Duc & Emsellem 2008) or protogalactic fragments seems to be the more likely explanation for the formation of even the lowest metallicity globular clusters.

We also find a slightly larger than expected velocity dispersion in the central regions of the cluster, which might point to a significant binary fraction or additional unseen matter in the core. At the same time, the rather low velocity dispersion in the outer regions of the cluster could pose a problem for alternative gravitational theories like MOND. These conclusions rely on several assumptions that we had to make for our modelling, in particular that stellar orbits are isotropic throughout the cluster and that the stellar M/L is constant with radius. Acquiring additional radial velocities would help test the validity of these assumptions and strengthen our conclusions.

ACKNOWLEDGMENTS

We thank Tad Pryor and Ed Olszewski for providing their finding charts for NGC 2419. We also thank Iskren Georgiev and an anonymous referee for comments which improved the presentation of the paper. This study was based on observations obtained at the W. M. Keck Observatory, which is operated jointly by the California Institute of Technology and the University of California. We are grateful to the W. M. Keck Foundation for their vision and generosity. SGD acknowledges a partial support from the NSF grant AST-0407448, and the Ajax Foundation.

REFERENCES

Ashman K. M., Zepf S. E., 1992, ApJ, 384, 50
Baumgardt H., Mieske S., 2008, MNRAS, 391, 942
Baumgardt H., Makino J., Hut P., 2005, ApJ, 620, 238
Bellazzini M., 2007, A&A, 473, 171
Binney J., Tremaine S., 1987, Galactic Dynamics. Princeton Univ. Press, Princeton, NJ
Bournaud F., Duc P. A., Emsellem E., 2008, MNRAS, 389, 8
Bruzual A. G., Charlot S., 2003, MNRAS, 344, 1000
Cen R., 2001, ApJ, 560, 592
Chabrier G., 2003, PASP, 115, 763
Côté P., Mateo M., Olszewski E. W., Cook K. H., 1999, ApJ, 526, 147
Côté P., Djorgovski S. G., Meylan G., Castro S., McCarthy J. K., 2002, ApJ, 574, 783
Côté P. et al., 2007, ApJ, 671, 1456
Dabringhausen J., Hilker M., Kroupa P., 2008, MNRAS, 386, 864
Dabringhausen J., Kroupa P., Baumgardt H., 2009, MNRAS, 394, 1529
Dalessandro E., Lanzoni B., Ferraro F. R., Vespe F., Bellazzini M., Rood R. T., 2008, ApJ, 681, 311
Djorgovski S., 1993, in Djorgovski S. G., Meylan G., eds, ASP Conf. Ser. Vol. 50, Structure and Dynamics of Globular Clusters. Astron. Soc. Pac., San Francisco, p. 373
Dotter A., Chaboyer B., Jevremović D., Kostov V., Baron E., Ferguson J. W., 2008, ApJS, 178, 89
Drinkwater M. J., Jones J. B., Gregg M. D., Phillipps S., 2000, Publ. Astron. Soc. Aust., 17, 227
Evstigneeva E. A., Gregg M. D., Drinkwater M. J., Hilker M., 2007, AJ, 133, 1722
Ferrarese L. et al., 2006, ApJS, 164, 334
Gilmore G., Wilkinson M. I., Wyse R. F. G., Kleyna J. T., Koch A., Evans N. W., Grebel E. K., 2007, ApJ, 663, 948
Goerdt T., Moore B., Kazantzidis S., Kaufmann T., Maccio A. V., Stadel J., 2008, MNRAS, 385, 2136
Goudfrooij P., Mack J., Kissler-Patig M., Meylan G., Minniti D., 2001, MNRAS, 322, 643
Graham A. W., Guzmán R., 2003, AJ, 125, 2936
Gunn J. E., Griffin R. F., 1979, AJ, 84, 752
Haghi H., Baumgardt H., Kroupa P., Grebel E. K., Hilker M., Jordi K., 2009, MNRAS, 395, 1549
Harris W. E., 1996, AJ, 112, 487
Harris W. E. et al., 1997, AJ, 114, 1030
Haşegan M. et al., 2005, ApJ, 627, 203
Hilker M., Infante L., Viera G., Kissler-Patig M., Richtler T., 1999, A&AS, 134, 75
Hilker M., Baumgardt H., Infante L., Drinkwater M., Evstigneeva E., Gregg M., 2007, A&A, 463, 119
Jordán A. et al., 2005, ApJ, 634, 1002
Jordi K. et al., 2009, AJ, 137, 4586
King I., 1962, AJ, 67, 471
Kravtsov A. V., Gnedin O. Y., 2005, ApJ, 650, 665
Kroupa P., 2001, MNRAS, 322, 231
Leon S., Meylan G., Combes F., 2000, A&A, 359, 907
Maraston C., 2005, MNRAS, 362, 799
Mashchenko S., Sills A., 2005, ApJ, 619, 258
Mayor M. et al., 1984, A&A, 134, 118
Mieske S. et al., 2008, A&A, 487, 921
Milgrom M., 1983a, ApJ, 270, 365
Milgrom M., 1983b, ApJ, 270, 371
Milgrom M., 1994, ApJ, 429, 540
Murray N. W., 2009, ApJ, 691, 946
Olszewski E. W., Pryor C., Schommer R. B., 1993, in Smith G. H., Brodie J. P., eds, ASP Conf. Ser. Vol. 48, The Globular Clusters–Galaxy Connection. Astron. Soc. Pac., San Francisco, p. 99
Peebles P. J. E., 1984, ApJ, 277, 470
Pryor C., Meylan G., 1993, in Djorgovski S., Meylan G., eds, ASP Conf. Ser. Vol. 50, Structure and Dynamics of Globular Clusters. Astron. Soc. Pac., San Francisco, p. 357

Racine R., Harris W. E., 1975, ApJ, 196, 413
Rejkuba M., Dubath P., Minnit D., Meylan G., 2007, A&A, 469, 147
Ripepi V. et al., 2007, ApJ, 667, L61
Robin A. C., Reylé C., Derriére S., Picaud S., 2003, A&A, 409, 523
Salaris M., Weiss A., 2002, A&A, 388, 492
Sanders R. H., McGaugh S. S., 2002, ARA&A, 40, 263
Searle L., Zinn R., 1978, ApJ, 225, 357
Sérsic J. L., 1963, Bol. Asoc. Argentina Astron., 6, 41
Shetrone M. D., Côté P., Sargent W. L. W., 2001, ApJ, 548, 592
Strigari L. E., Bullock J. S., Kaplinghat M., Diemand J., Kuhlen M., Madau P., 2008, AJ, 669, 676
Tonry J., Davis M., 1979, AJ, 84, 1511
Trager S. C., King I. R., Djorgovski S., 1995, AJ, 109, 218
van de Ven G., van den Bosch R. C. E., Verolme E. K., de Zeeuw P. T., 2006, A&A, 445, 513
Vogt S. S. et al., 1994, Proc. SPIE, 2198, 362
Vogt S. S., Mateo M., Olszewski E. W., Keane M. J., 1995, AJ, 109, 151
Walker M. G., Mateo M., Olszewski E. W., Gnedin O. Y., Wang X., Sen B., Woodroofe M., 2007, ApJ, 667, 53
West M. J., 1993, MNRAS, 265, 755
Whitmore B. C., Schweizer F., 1995, AJ, 109, 960
Whitmore B. C., Zhang Q., Leitherer C., Fall S. M., Schweizer F., Miller B. W., 1999, AJ, 118, 1551
Wu X., 2007, ApJ, submitted (astro-ph/0702233v1)

This paper has been typeset from a TEX/LATEX file prepared by the author.